Green Synthesis of AuNPs Using *Ocimum Basilicum* Extract and Study of Its Potential as Microplastic Detection

Muhammad Bakhru Thohir [a,1,*], Aan Ma'ruf Ainnurokhim Wijaya [a,2], Anggi Tri Nurhaliza [a,3], Mochamad Suud [a,4]

[a] Department of Chemistry, Faculty of Science and Engineering, Universitas Bojonegoro, Bojonegoro, Indonesia
[1] bakhru@unigoro.ac.id*; [2] aan005527@gmail.com; [3] nuranggi64@gmail.com; [4] Msuudmbling@gmail.com
* corresponding author

ARTICLE INFO

Article history
Received November 7, 2025
Revised June 7, 2026
Accepted June 8, 2026

Keywords
AuNPs
Environmental Monitoring
Green Synthesis
Microplastics
Ocimum Basilicum

ABSTRACT

Nanoparticles have emerged as promising materials for real-time environmental monitoring due to their unique optical and physicochemical properties. Among them, gold nanoparticles (AuNPs) have gained considerable attention for sensing applications, including the detection of emerging pollutants such as microplastics. However, conventional AuNP synthesis commonly relies on hazardous chemicals and energy-intensive processes, creating environmental and sustainability concerns. Therefore, the development of green synthesis methods using plant-based bioreductors offers a more sustainable alternative. This study aims to determine the optimal conditions for the green synthesis of AuNPs using Ocimum basilicum extract, characterize the synthesized nanoparticles, and evaluate their potential application for microplastic detection. The research involved the extraction of Ocimum basilicum, optimization of synthesis parameters, nanoparticle characterization, and assessment of microplastic monitoring capability. The results showed that stable AuNPs were successfully synthesized under optimum conditions at pH 6 with a precursor-to-bioreductor ratio of 6:3 (mL). The synthesized AuNPs-OB exhibited an average particle size of 3.52 nm, indicating the formation of small and highly reactive nanoparticles. Fourier Transform Infrared (FTIR) analysis revealed the presence of hydroxyl (O–H) and alkene (C=C) functional groups originating from Ocimum basilicum phytochemicals, which contributed to both the reduction and stabilization of the nanoparticles. Furthermore, AuNPs-OB demonstrated promising potential for microplastic detection through direct and indirect approaches. The direct method involved surface modification with non-polar compounds to enhance interactions with microplastics, while the indirect method employed acetone as an aggregating agent to induce detectable optical changes. These findings demonstrate that green-synthesized AuNPs-OB are environmentally friendly nanomaterials with strong potential for sustainable microplastic monitoring applications.

1. Introduction

Those of us living today need to consider those who will inhabit the planet in the future. While we currently enjoy a relatively healthy environment, future generations also deserve the same privilege. Environmental activists have long championed this ideal, yet it appears increasingly difficult to achieve given the current trajectory of environmental degradation. Historically persistent pollutants—such as oil spills, surfactants, pesticides, and heavy metals—have not been fully addressed. Worse still, we are now confronted with newer pollutants that pose even more insidious threats, such as microplastics [1].

Microplastics result from the slow degradation of plastic. In modern life, plastic is ubiquitous due to its multipurpose nature: it is flexible, waterproof, and durable. Ironically, these advantageous properties also contribute to its resistance to degradation [2]. Even at the nanoscale, plastics retain their original characteristics, which becomes problematic when plants, animals, or humans ingest microplastics. Their presence can disrupt biological systems, for instance, by inducing fat agglomeration that interferes with metabolism [3], [4]. Additionally, the porous structure of microplastics enables them to adsorb heavy metals, which may then enter biological organisms [5].

Given the complexity of this issue, monitoring water quality to detect microplastic contamination is critical. Currently, such monitoring is carried out using instrumental techniques like SEM, FTIR, and Raman spectroscopy [6]. While effective, these methods are slow, expensive, require trained personnel, and are energy-intensive [7]. Consequently, alternative approaches are needed—ones that are simple, low-cost, environmentally friendly, and capable of delivering rapid detection.

Gold nanoparticles (AuNPs) have emerged as promising candidates for addressing the challenge of microplastic detection. This is due to their unique properties, including small size, tunable surfaces, large surface area, and distinct optical features [8]. AuNPs have been widely used for colorimetric detection in applications ranging from water quality monitoring to cancer diagnostics [9].

However, conventional synthesis methods for AuNPs are not environmentally sustainable. They often rely on synthetic chemicals, excessive use of raw materials, and harsh reaction conditions. Ascorbic acid and sodium citrate are typically employed as reducing agents, and stabilizers are also required, making the process resource-intensive [10]. To address this issue, green synthesis methods utilizing bioreductants have been proposed [11].

Green synthesis of AuNPs employs reducing agents derived from natural sources such as plant extracts, bacteria, or fungi [12]. Plants are particularly suitable as bioreductants due to their abundance of secondary metabolites that facilitate electron transfer and reduction reactions [13]. Extracts rich in phenolics, saponins, tannins, and flavonoids can serve dual roles—as reducing agents and stabilizers—enhancing the sustainability of the synthesis process [12].

Several successful syntheses of AuNPs have been reported using extracts from *Curcuma pseudomontana*, *Capsicum annum*, and *Zingiber officinale*. These biogenic AuNPs have demonstrated various bioactivities, including antimicrobial, anti-inflammatory, and antioxidant effects [12], [14], [15]. However, green-synthesized AuNPs also exhibit immense potential as sensors, owing to their unique optical behaviors. These nanoparticles can shift their absorption wavelength as their size changes. Moreover, their agglomeration capability induces detectable color changes, which can be harnessed for simple detection methods [11]. Surface modification with non-polar compounds also enables both direct and indirect detection of microplastics [17].

Ocimum basilicum stands out as a plant with strong potential as a bioreductant [16]. *Ocimum basilicum* makes it a strong candidate for use in nanoparticle synthesis, especially considering its richness in phytosterols, alkaloids, phenolics, lignins, tannins, starches, saponins, flavonoids, and terpenoids—all of which are relevant to the reduction process [16]. Notably, no previous reports have described the synthesis of AuNPs using *Ocimum basilicum* for microplastic detection, suggesting a promising research opportunity.

Therefore, the objectives of this study were to determine the optimal synthesis conditions for green AuNPs using *Ocimum basilicum* by varying the pH and precursor-to-reducing agent ratios, to characterize the physicochemical properties of the synthesized nanoparticles, and to evaluate the theoretical potential of these AuNPs as a future microplastic detector. The novelty of this research lies in introducing a new green synthesis approach using Ocimum basilicum and investigating the resulting AuNPs for microplastic detection.

2. Research Methodology

2.1. Materials

The materials required for the study comprised *Ocimum basilicum* (basil) leaf powder, distilled water, pure gold metal, hydrochloric acid (HCl, 37%), and nitric acid (HNO_3, 65%).

The instruments used in this study included a UV–Visible spectrophotometer (Agilent Technologies Cary 60), Fourier Transform Infrared Spectroscopy (FTIR, Agilent Technologies), Particle Size Analyzer (PSA, Malvern Panalytical), hot plate, thermometer, stopwatch, glass vials, filter paper, Büchner funnel, stirring rod, analytical balance, and a complete set of standard laboratory glassware.

2.2. Procedures

1) Extraction of Ocimum basilicum Leaf

A total of 0.075 g of dried *Ocimum basilicum* leaf powder was weighed and added to 100 mL of boiling distilled water. The extraction was carried out for 10 minutes without stirring. The resulting extract was filtered using a Büchner funnel with vacuum filtration. The filtrate was stored in a refrigerator for two weeks and regenerated before use.

2) Preparation $HAuCl_4$ Precursor

$HAuCl_4$ precursor solution was prepared by dissolving 0.1 g of pure gold metal in a 3:1 (v/v) mixture of concentrated HCl (37%) and HNO_3 (65%). The reaction was conducted under closed conditions in a fume hood for 48 hours. The resulting solution was heated to evaporate, yielding solid HAuCl4, which was subsequently dissolved in distilled water to a final volume of 100 mL, yielding a final concentration of 5.07 mM.

3) pH Optimization of AuNPs-OB Synthesis

The pH optimization was carried out by first adjusting the *Ocimum basilicum* extract (0.075% w/v) to the target pH values (2, 4, 6, 8, and 12) using HCl for acidic conditions and NaOH for alkaline conditions. Then, 3 mL of each adjusted extract was mixed with 6 mL of 5.07 mM $HAuCl_4$ solution under boiling conditions. The reaction was maintained under a boil for 10 minutes, followed by additional stirring at room temperature for 10 minutes.

4) Optimization of Precursor-to-Bioreductant Ratio

The optimization of the volume ratio between the gold precursor and *Ocimum basilicum* extract was performed using the same procedure as the pH optimization, with the previously determined optimum pH applied. The ratios tested (in mL) were 12:3, 12:6, 6:3, 6:6, and 6:12 (precursor:bioreductant).

5) Characterization of AuNPs-OB and Study of Potential for Microplastic Detection

The synthesized AuNPs-OB were characterized using UV–Visible spectroscopy in the wavelength range of 300–800 nm to determine the optimum synthesis conditions. Functional group analysis was conducted using FTIR in the wavenumber range of 4000–400 cm^{-1}. Particle size distribution was analyzed using a Particle Size Analyzer (PSA). Furthermore, their potential for microplastic detection was evaluated theoretically through a comprehensive literature review. To support this assessment, initial aggregation experiments were carried out using acetone as the medium.

3. Results and Discussion

Gold nanoparticles (AuNPs) represent a modern scientific advancement that significantly influences technological progress. Owing to their unique physicochemical characteristics, nanoparticles have reshaped conventional scientific understanding [8]. Traditionally, the properties of a substance were primarily attributed to its valence electrons; however, at the nanoscale, these properties are also determined by particle size [18]. This paradigm shift underscores the exceptional behavior of nanomaterials, which exhibit attributes such as a high surface area-to-volume ratio, tunable magnetic properties, nanoscale dimensions, and surface modifiability. These features have led to their widespread application in medical treatments, optical technologies, and environmental monitoring [19].

In particular, AuNPs have great potential for detecting emerging environmental pollutants, such as microplastics, which pose a growing threat to ecosystem stability. Due to their hydrophobic nature, microplastics can be targeted with detection strategies involving surface-modified nanoparticles. By modifying the AuNP surface to be hydrophobic, it is possible to induce interactions with microplastics, enabling detection via precipitation or colorimetric responses [20]. However, to ensure reliable detection performance, it is crucial first to establish the optimal synthesis conditions that yield AuNPs with suitable size and stability for further use as microplastic sensors.

3.1. Synthesis of AuNPs at Varied pH

The synthesis of gold nanoparticles (AuNPs) began with the extraction of *Ocimum basilicum* using boiling water without stirring, yielding a plant extract that served as a bioreductant. The application of heat during extraction facilitated the breakdown of plant cell walls and the release of secondary metabolites [21]. Concurrently, the gold precursor ($HAuCl_4$) was prepared by digesting pure gold metal in aqua regia. Following the dissolution, the solution was evaporated to yield solid $HAuCl_4$ salt [22]. Once both components were ready, the synthesis was initiated.

The initial stage involved optimizing the pH conditions for the synthesis. The $HAuCl_4$ solution was brought to a boil under continuous stirring. The heating process provided sufficient kinetic energy for the gold precursor to overcome the activation energy barrier required for nanoparticle formation [10]. Stirring was applied to maintain a homogeneous reaction medium [23]. Separately, the pH of the *O. basilicum* extract was adjusted to 2, 4, 6, 8, and 12. Varying the pH alters the ionization state of the extract's secondary metabolites, affecting their ability to reduce Au ions [24]. At this stage, the $HAuCl_4$ solution appeared pale yellow, while the extract was turbid green.

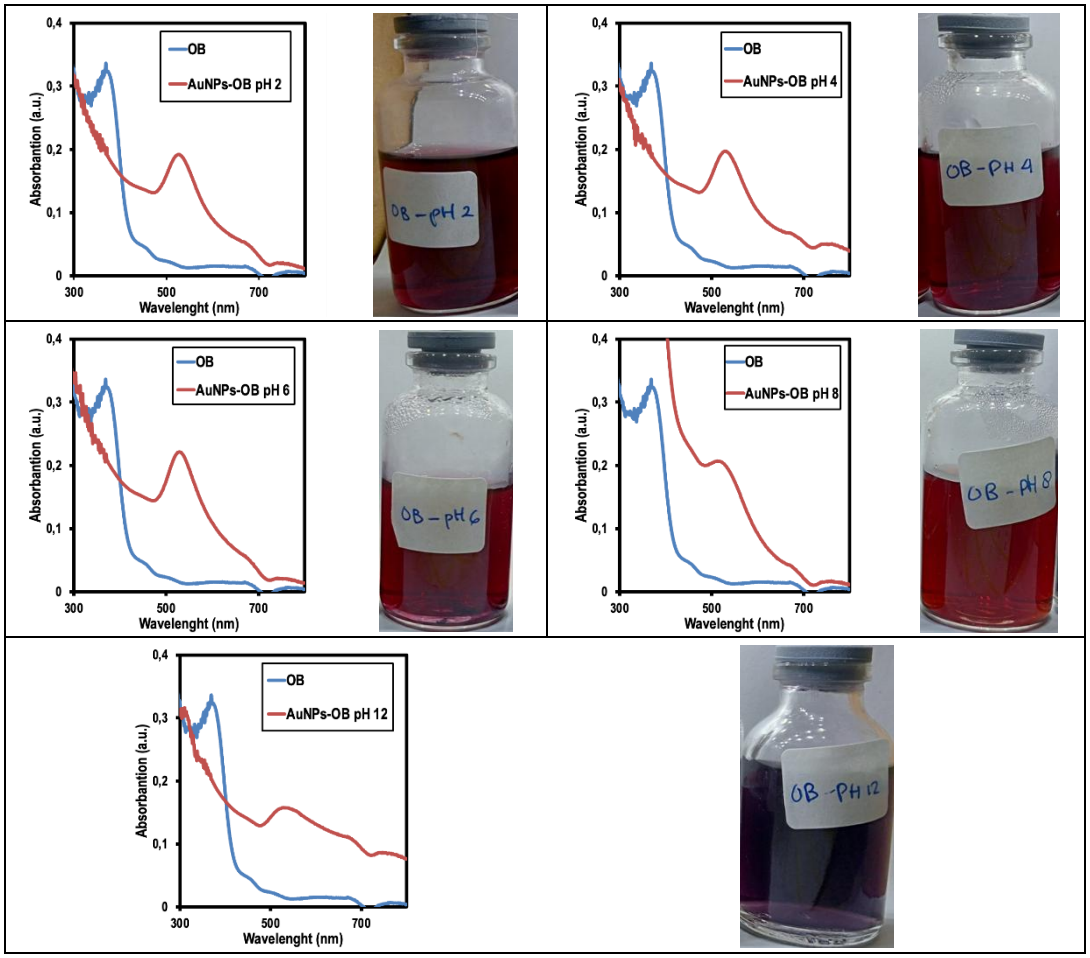

Fig. 1. Synthesis outcomes of AuNPs-OB under varying pH conditions of the reducing agent. (left) UV-Visible absorption spectra of the synthesized AuNPs; (right) corresponding visual appearance of the AuNPs-OB.

The synthesis was carried out for 10 minutes under boiling conditions, followed by an additional 10 minutes of stirring without heating to allow gradual cooling and complete nanoparticle formation [12]. Experimental observations revealed that pH values of 2, 4, 6, and 8 successfully yielded AuNPs, indicated by the formation of a burgundy (wine-red) color. In contrast, under highly alkaline conditions (pH 12), AuNP formation was inhibited, evidenced by a purple solution. A red color typically signifies the formation of nanoscale AuNPs, whereas a purple hue suggests the presence of larger, aggregated particles beyond the nanoscale [25].

UV-Visible spectrophotometry was employed to confirm AuNP formation. At pH 2, a characteristic absorption peak appeared at around 520 nm—an indicative surface plasmon resonance (SPR) signal for AuNPs. However, the peak intensity was relatively low, suggesting limited nanoparticle formation. Stronger, narrower SPR peaks were observed at pH 4 and pH 6, indicating higher yields of AuNPs with a more uniform particle-size distribution. A narrower peak typically correlates with improved monodispersity [26].

At pH 8, visual observation still indicated a wine-red color, suggesting nanoparticle formation. However, spectral analysis revealed a broader, less intense SPR band, indicative of a lower particle concentration and increased size heterogeneity. At pH 12, neither color change nor a distinct SPR peak was detected, confirming the absence of AuNP formation [27]. These results are presented in Fig. 2.

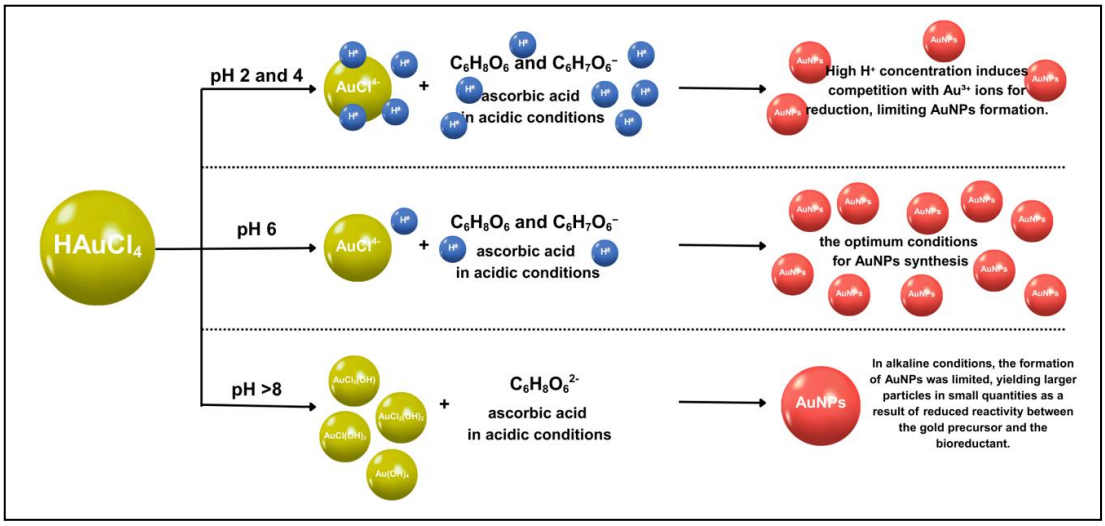

Fig. 2. Simulation of AuNPs synthesis under various pH conditions.

From these findings, it can be concluded that pH 6 is the optimal condition for the synthesis of AuNPs using *O. basilicum* extract. In general, AuNPs synthesis mediated by *O. basilicum* bioreductant favors mildly acidic conditions. Under such conditions, the gold precursor predominantly exists as $AuCl_4^-$, a form highly susceptible to reduction [28]. In contrast, basic conditions promote ligand substitution of chloride ions with hydroxide, forming complexes such as $AuCl_3(OH)$, $AuCl_2(OH)_2$, $AuCl(OH)_3$, and $Au(OH)_4^-$, which are significantly more stable and less reactive [24].

Moreover, the reactivity of secondary metabolites is also influenced by pH. Under acidic conditions, reducing agents such as ascorbic acid predominantly exist in the protonated forms ($C_6H_8O_6$ and $C_6H_7O_6^-$), which exhibit strong electron-donating ability. Conversely, in alkaline environments, ascorbic acid is deprotonated to $C_6H_6O_6^{2-}$, which is considerably less reactive [29]. Therefore, mildly acidic conditions provide an optimal environment in which both the precursor and the reducing agent are in their most reactive states. Nevertheless, extremely low pH values (very high H^+ concentrations) may also hinder reduction efficiency due to competitive interactions between H^+ and Au^{3+} ions, thereby suppressing nucleation and limiting nanoparticle formation [30].

Overall, pH 6 enables effective reduction of $AuCl_4^-$ without interference from excessive proton concentration, allowing stable and uniform AuNP formation. These findings are consistent with previous studies [31], which reported that optimal AuNP synthesis using bioreductants typically occurs under mildly acidic to neutral conditions (pH 6–8).

3.2. Synthesis of AuNPs with Variations in Precursor: Bioreductant Ratios

This stage followed the same procedure as the previous experiment, using the optimized pH of 6 for the bioreductant. The volumes of precursor and bioreductant were varied at 12:3, 12:6, 6:3, 6:6, and 6:12 (mL). Unlike during the pH optimization stage, visual observation indicated successful formation of AuNPs across all ratio variations, as evidenced by the consistent appearance of a wine-red color. However, UV-Visible spectrophotometry revealed contrasting results. AuNP formation occurred only in variations with a higher proportion of gold precursor. In conditions where the

precursor amount was equal to or less than the bioreductant, no AuNP formation was observed (Fig. 3).

In the 12:3 variation, a dark red color was observed. The UV-Vis spectrum showed that although a large quantity of AuNPs was formed, the size distribution was heterogeneous. A high concentration of precursor increases the likelihood of nanoparticle formation [32]. However, the limited amount of bioreductant may not be sufficient to fully reduce the available gold ions. Consequently, some unreduced Au^{3+} ions may act as ionic bridges between nanoparticle surfaces, leading to particle aggregation and an increased average particle size [33]. This leads to the coexistence of both free-standing AuNPs and those interconnected via Au^{3+} ion bridges, contributing to the observed size non-uniformity. Moreover, the insufficient amount of bioreductant also implies fewer stabilizing agents, further promoting agglomeration [34].

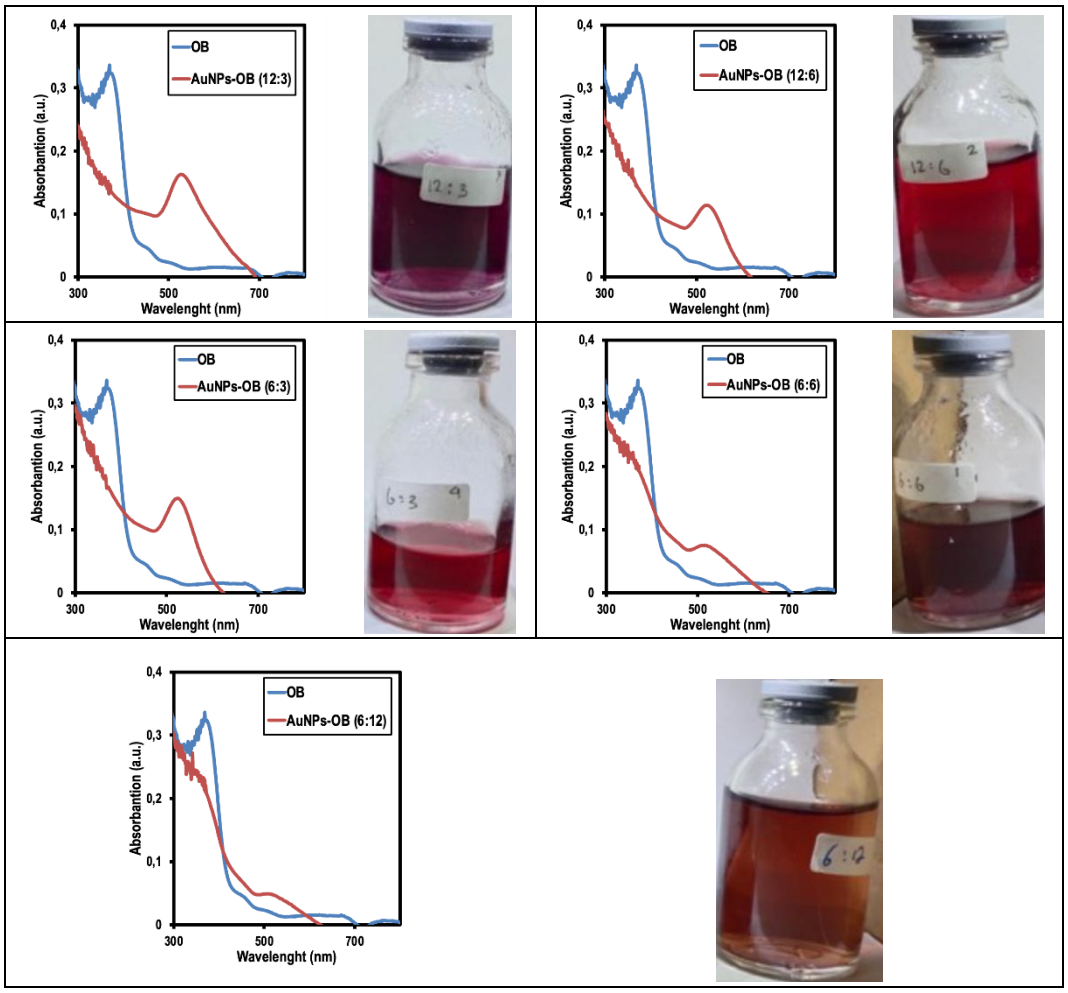

Fig. 3. Synthesis outcomes of AuNPs-OB under varying precursor-to-reducing agent ratios. (left) UV-Visible absorption spectra of the synthesized AuNPs; (right) corresponding visual appearance of the AuNPs-OB.

The most favorable synthesis conditions were obtained at precursor:bioreductant ratios of 12:6 and 6:3. These variations produced vivid red solutions, and their UV-Vis spectra showed sharp and narrow peaks, indicating the formation of uniform and monodisperse AuNPs [35]. However, an unexpected finding emerged: despite the same ratio, the larger absolute volume (12:6) yielded fewer nanoparticles than the smaller one (6:3).

This phenomenon can be interpreted using the concept of reaction kinetics. One of the factors influencing reaction rate is the concentration of the reactants. Higher precursor concentrations can accelerate the reduction process; however, excessive speed may lead to uncontrolled nucleation and aggregation [36]. In such cases, rapid particle growth may prevent the formation of stable and well-dispersed nanoparticles due to steric crowding and insufficient stabilization.

On the other hand, when higher amounts of bioreductant were used, as seen in the 6:6 and 6:12 ratios, the resulting colors became progressively lighter—from pale red to orange. This color change was corroborated by the UV-Vis spectra, where the characteristic absorption peak around 520 nm, typically associated with AuNPs, diminished or disappeared. These observations indicate that AuNPs were either not formed or formed in very low quantities.

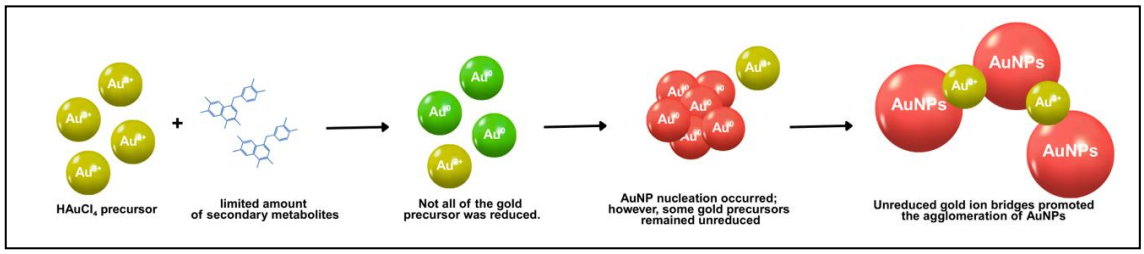

Fig. 4. Schematic illustration of AuNP agglomeration induced by unreduced gold ion bridging.

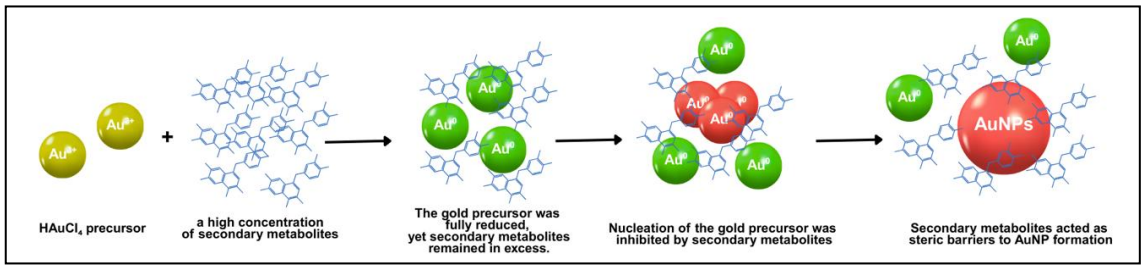

Fig. 5. Schematic representation of AuNP formation failure due to steric hindrance by excess secondary metabolites.

This outcome can be attributed to an excessive amount of bioreductant, which causes the precursor to be reduced too rapidly. Such rapid reduction leads to immediate core agglomeration, preventing proper nucleation and nanoparticle formation. Moreover, an excess of reducing agent may act as a steric hindrance, physically obstructing the gold atoms from assembling into stable nanoparticle structures [37].

Based on these findings, the optimal ratio for AuNP synthesis using *O. basilicum* extract is 6:3 (mL). This result aligns with previous research [38], which reported that nanoparticle size and yield can be effectively controlled by adjusting the precursor-to-reducing-agent ratio during green synthesis protocols.

3.3. AuNPs-OB Characterization: FTIR and PSA

1) FTIR

Fourier Transform Infrared Spectroscopy (FTIR) was employed to identify functional groups interacting with metal particles and biomolecules [39]. The FTIR spectrum of the *Ocimum basilicum* extract showed characteristic peaks at 3265.1 cm^{-1}, 2124.6 cm^{-1}, 2001.6 cm^{-1}, and 1636.3 cm^{-1}. In contrast, AuNPs synthesized using *Ocimum basilicum* (AuNPs-OB) displayed peaks at 3261.4 cm^{-1}, 2128.3 cm^{-1}, and 1636.3 cm^{-1}.

The bands around 3265.1 cm^{-1} and 3261.4 cm^{-1} are attributed to O–H stretching vibrations, indicating the presence of hydroxyl groups. This observation aligns with findings from [40], which reported that polyphenolic compounds in green tea leaves exhibit strong O–H stretching in the 3600–3200 cm^{-1} region.

A distinct absorption band at 1636.3 cm^{-1} was observed in both the extract and AuNPs-OB samples, suggesting the presence of C=C stretching vibrations. This is consistent with the results obtained by Mardina *et al.* [41], who identified a similar band at 1626.85 cm^{-1} in AuNPs synthesized using cinnamon essential oil.

Additionally, absorption bands in the 2000–2130 cm^{-1} range (specifically at 2124.6 cm^{-1}, 2128.3 cm^{-1}, and 2001.6 cm^{-1}) may correspond to C≡C stretching vibrations, indicating the presence of alkyne groups. [42] Similarly, it was reported that alkyne ester functional groups absorb within the 2260–2000 cm^{-1} range.

Phytochemicals such as monoterpenoids, sesquiterpenes, and phytol in *O. basilicum*—which contain hydroxyl (O–H) and alkene (C=C) groups—are known to function as both reducing and stabilizing agents by binding to Au^{3+} ions. However, it is important to note that the FTIR data obtained in this study do not exhibit strong shifts or the emergence of new peaks that are typically associated with Au–functional group interactions. This may be attributed to the limitations of mid-infrared FTIR, which covers only the wavenumber range of 400–4000 cm^{-1} [43]. Furthermore, it suggests that the stabilizing capping layer is weakly bound via physical adsorption (physisorption) rather than through strong covalent interactions that would significantly perturb the original peak positions.

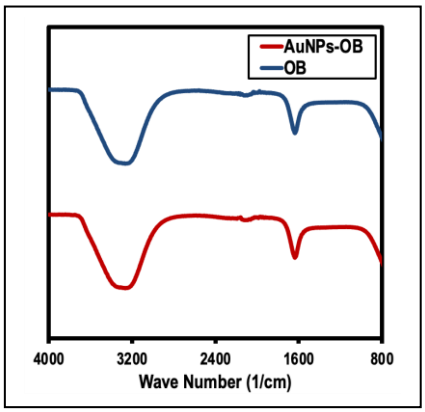

Fig. 6. FTIR spectra of *Ocimum basilicum* extract and synthesized AuNPs-OB.

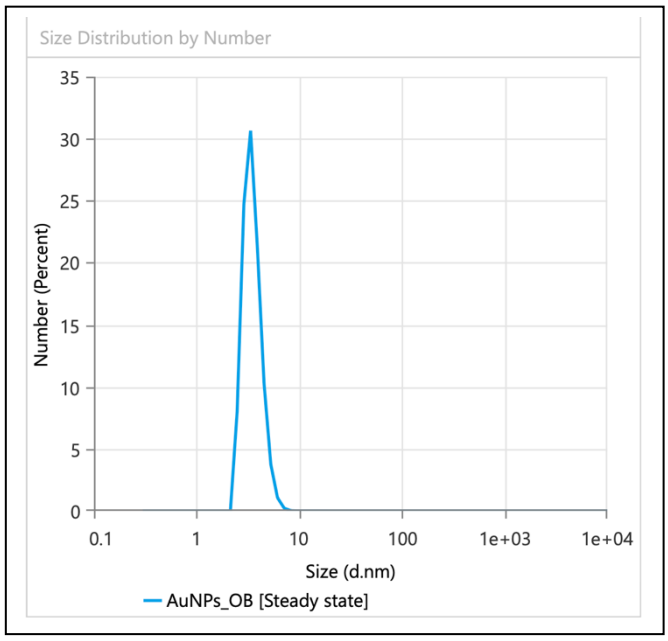

Fig. 7. PSA results of AuNPs-OB synthesized using *Ocimum basilicum* extract.

Table 1. PSA Data of Green-Synthesized AuNPs-OB

Data	Value (Average)
Peak 1, mean size (nm)	3.519
Peak 1, percentage size (%)	99.98
Peak 2, mean size (nm)	15.44
Peak 2, percentage size (%)	0.01917

2) PSA

Particle Size Analyzer (PSA) was utilized to determine the size distribution of AuNPs-OB [44], using samples synthesized under optimal conditions (pH 6 and precursor:bioreductant ratio of 6:3). The average particle size was found to be 3.519 nm. This result is highly satisfactory, as it demonstrates that *O. basilicum* extract—despite being a natural bioreductant—was capable of

synthesizing ultra-small, well-dispersed nanoparticles. As summarized in Table 2, the particle size is well within the nanoscale range (1–100 nm), confirming the successful formation of AuNPs.

3.4. Study of the Potential of AuNPs-OB as a Colorimetric Detector for Microplastics

The application of gold nanoparticles (AuNPs) for the colorimetric detection of microplastics represents a novel, underexplored approach, particularly when the nanoparticles are synthesized using environmentally friendly methods. AuNPs exhibit significant potential as agents for environmental monitoring, as demonstrated by Zhao and Hong in their studies on microplastic detection using nanoparticles [45], [46].

In this context, two analytical strategies are commonly referenced: the direct and indirect detection methods. The direct method involves interaction between AuNPs and microplastics, leading to physicochemical changes—most notably, a visible color change. This approach leverages the inherent hydrophobicity of microplastics. Because microplastics are hydrophobic, they can interact with similarly hydrophobic-modified nanoparticles in a "like dissolves like" manner [47], [48]. In the study [45], for instance, AuNPs were surface-modified with hydrophobic protein moieties. Upon contact with microplastics, dipole–dipole interactions triggered nanoparticle aggregation, thereby increasing their size. This change in size alters the surface plasmon resonance of the particles, causing a noticeable color shift from red to purple (Fig. 8).

Conversely, the indirect method employs an external agent—such as acetone—to induce nanoparticle aggregation. Acetone acts as a molecular aggregator that gradually changes the color of AuNPs from red to blue as its concentration increases [10], [49]. This occurs due to an increase in particle size caused by aggregation. However, in the presence of microplastics, the particles act as a steric barrier, obstructing the aggregation process. As a result, the solution retains its original red color, indicating the presence of microplastics (Fig. 9).

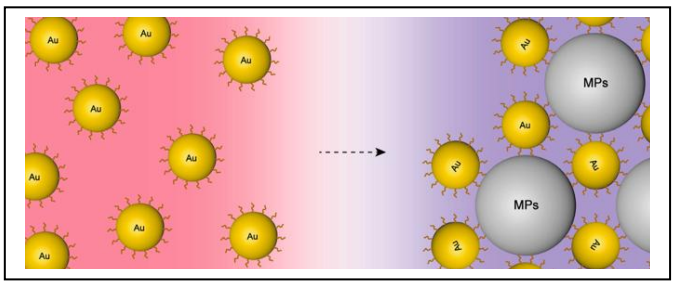

Fig. 8. Schematic of colorimetric interaction between modified AuNPs and microplastics [45].

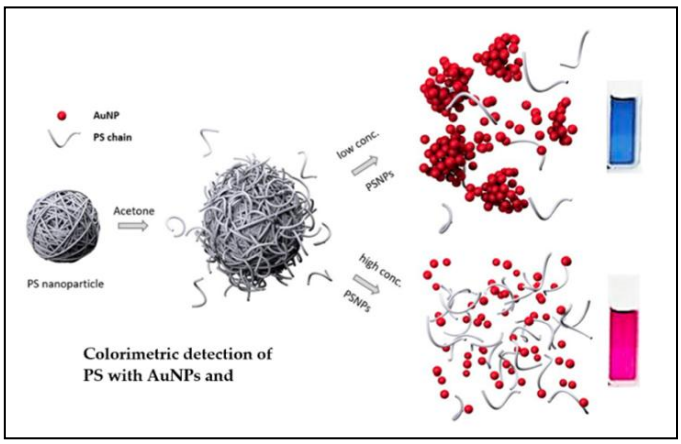

Fig. 9. Schematic of AuNP-based microplastic detection assisted by acetone aggregation [46].

These two colorimetric approaches offer promising alternatives to conventional instrumentation such as Raman spectroscopy, FTIR, and SEM, particularly for their simplicity, speed, and low operational cost. Viewed through the lens of the 12 Principles of Green Chemistry, this method offers multiple advantages over traditional instrumentation-based approaches. First, it significantly reduces energy consumption. While conventional instruments demand substantial energy input across various stages—including sampling, analysis, and data processing—the colorimetric method requires only

minimal energy, limited to the nanoparticle synthesis phase [50]. Second, the process itself is straightforward and inherently safe. The synthesis is conducted under mild conditions, without the involvement of hazardous reagents or extreme reaction environments [51]. Third, the use of naturally derived bioreductants—such as *Ocimum basilicum* extract—enhances the environmental friendliness of the synthesis by avoiding reliance on synthetic chemicals and promoting the use of renewable resources [52]. Finally, the application of this method to real-time, in situ environmental monitoring directly supports the eleventh principle of green chemistry, which emphasizes the design of safer analytical methodologies that minimize pollution at the source [53].

Table 2. PSA Data of Green-Synthesized AuNPs-OB

Type of Nanoparticle	Bioreductant	Particle Size (nm)	Reference
gold nanoparticles	Jatropha integerrima	38.8	[54]
gold nanoparticles	Curcuma pseudomontana	20.0	[15]
gold nanoparticles	Capsicum annum	20.0-30.0	[12]
gold nanoparticles	Ocimum basilicum	3.52	This work

In summary, this study not only introduces an environmentally benign synthesis of AuNPs but also demonstrates their promising utility in the real-time detection of microplastics. The integration of green synthesis with innovative analytical applications marks a significant step forward in both nanomaterials research and sustainable environmental monitoring.

4. Conclusion

This study successfully demonstrated the green synthesis of gold nanoparticles (AuNPs) using *Ocimum basilicum* extract as a bioreductant. The optimal synthesis conditions were established at pH 6 with a precursor-to-reducing agent ratio of 6:3 (mL). Characterization results confirmed the successful formation of AuNPs through visual color changes, UV-Visible spectrophotometry, FTIR analysis, and particle size analysis (PSA). The synthesized colloid exhibited a distinct red coloration, with a maximum absorption wavelength around 520 nm, which is characteristic of AuNPs. FTIR analysis indicated the presence of functional groups associated with polyphenolic and terpenoid compounds, supporting the role of *Ocimum basilicum* metabolites as effective reducing and stabilizing agents. PSA measurements showed a nanoparticle size of approximately 3.52 nm, indicating not only successful formation of nanosized particles but also high monodispersity and stability, despite the use of natural extract-based synthesis. These findings highlight the feasibility of using plant-derived bioreductants in green nanotechnology and offer a sustainable alternative to conventional chemical synthesis routes. Moreover, this work advances the application of biosynthesized AuNPs in environmental monitoring, particularly as a potential colorimetric sensor for microplastics. Further studies are recommended to explore the effects of additional synthesis variables, including extraction temperature, synthesis temperature, and reaction duration. Additional characterization techniques, such as transmission electron microscopy (TEM), are also suggested to further confirm the morphology and size distribution of the AuNPs-OB synthesized in this study. Additionally, future studies should investigate surface modification with non-polar compounds alongside comprehensive colorimetric or aggregation assays.

Acknowledgment

We gratefully acknowledge Universitas Bojonegoro, through its Research and Community Service Institute. We also extend our appreciation to the Chemistry Study Program students of the 2022 cohort who contributed to the green synthesis of AuNPs as part of their Instrumentation Practicals course project.

References

[1] L. Zhu, Y. Kang, M. Ma, Z. Wu, L. Zhang, R. Hu, Q. Xu, J. Zhu, X. Gu, and L. An, "Tissue accumulation of microplastics and potential health risks in human," *Science of the Total Environment*, vol. 915, pp. 170004, Mar 2024, doi: 10.1016/j.scitotenv.2024.170004.

[2] A. Prajapati, A. Narayan Vaidya, and A. R. Kumar, "Microplastic properties and their interaction with hydrophobic organic contaminants: a review," *Environmental Science and Pollution Research*, vol. 29, no. 33, pp. 49490–49512, Jul 2022, doi: 10.1007/s11356-022-20723-y.

[3] J.-B. Fleury and V. A. Baulin, "Microplastics destabilize lipid membranes by mechanical stretching," *Proceedings of the National Academy of Sciences*, vol. 118, no. 31, Aug 2021, doi: 10.1073/pnas. 2104610118.

[4] M. Yang, B. Zhang, X. Xin, B. Liu, Z. Zhu, G. Dong, Y. Zhao, K. Lee, and B. Chen, "Microplastic-oil-dispersant agglomerates in the marine environment: Formation mechanism and impact on oil dispersion," *J Hazard Mater*, vol. 426, pp. 127825, Mar 2022, doi: 10.1016/j.jhazmat.2021.127825.

[5] R. Kumar, N. Ivy, S. Bhattacharya, A. Dey, and P. Sharma, "Coupled effects of microplastics and heavy metals on plants: Uptake, bioaccumulation, and environmental health perspectives," *Science of the Total Environment*, vol. 836, pp. 155619, Aug 2022, doi: /10.1016/j.scitotenv.2022.155619.

[6] G. Alak, A. Uçar, V. Parlak, and M. Atamanalp, "Identification, characterisation of microplastic and their effects on aquatic organisms," *Chemistry and Ecology*, vol. 38, no. 10, pp. 967–987, Sep 2022, doi: 10.1080/02757540.2022.2126461.

[7] M. B. Thohir and W. P. K. Tiyas, "Colorimetric Sensor of Hg (II) Ion from AgNPs-MO Quantified Using DIC with ED Equation Approach," *Hydrogen: Jurnal Kependidikan Kimia*, vol. 12, no. 6, pp. 1389–1399, Dec 2024, doi: 10.33394/hjkk.v12i6.13772.

[8] K. A. Altammar, "A review on nanoparticles: characteristics, synthesis, applications, and challenges," *Front Microbiol*, vol. 14, pp. 1155622, Apr 2023, doi: 10.3389/fmicb.2023.1155622.

[9] H. H. Cho, D. H. Jung, J. H. Heo, C. Y. Lee, S. Y. Jeong, and J. H. Lee, "Gold nanoparticles as exquisite colorimetric transducers for water pollutant detection," *ACS Appl Mater Interfaces*, vol. 15, no. 16, pp. 19785–19806, Apr 2023, doi: 10.1021/acsami.3c00627.

[10] A. E. F. Oliveira, A. C. Pereira, M. A. C. Resende, and L. F. Ferreira, "Gold nanoparticles: a didactic step-by-step of the synthesis using the turkevich method, mechanisms, and characterizations," *Analytica*, vol. 4, no. 2, pp. 250–263, Jun 2023, doi: 10.3390/analytica4020020.

[11] M. B. Thohir, D. Setyaningrum, M. R. S. Efendi, A. A. Saputra, and M. C. Nursaida, "Synthesis AuNPs using moringa oleifera extract and potential study as colorimetric microplastic detection," *Jurnal Kependidikan Kimia*, vol. 13, no. 3, pp. 479–491, Jun 2025, doi: 10.33394/hjkk.v13i3.16603.

[12] T. P. Patil, A. A. Vibhute, S. L. Patil, T. D. Dongale, and A. P. Tiwari, "Green synthesis of gold nanoparticles via *Capsicum annum* fruit extract: Characterization, antiangiogenic, antioxidant and anti-inflammatory activities," *Applied Surface Science Advances*, vol. 13, Feb 2023, doi: 10.1016/j.apsadv.2023.100372.

[13] S. A. Akintelu, B. Yao, and A. S. Folorunso, "Green synthesis, characterization, and antibacterial investigation of synthesized gold nanoparticles (AuNPs) from Garcinia kola pulp extract," *Plasmonics*, vol. 16, no. 1, pp. 157–165, Feb 2021, doi: 10.1007/s11468-020-01274-9.

[14] A. Fouda, A. M. Eid, E. Guibal, M. F. Hamza, S. E. D. Hassan, D. H. M. Alkhalifah, and D. E. Hossary, "Green synthesis of gold nanoparticles by aqueous extract of zingiber officinale: characterization and insight into antimicrobial, antioxidant, and in vitro cytotoxic activities," *Applied Sciences (Switzerland)*, vol. 12, no. 24, Dec 2022, doi: 10.3390/app122412879.

[15] N. Muniyappan, M. Pandeeswaran, and A. Amalraj, "Green synthesis of gold nanoparticles using *Curcuma pseudomontana* isolated curcumin: Its characterization, antimicrobial, antioxidant and anti- inflammatory activities," *Environmental Chemistry and Ecotoxicology*, vol. 3, pp. 117–124, Jan 2021, doi: 10.1016/j.enceco.2021.01.002.

[16] V. T. Nguyen, N. Q. Nguyen, N. Q. N. Thi, C. Q. N. Thi, T. T. Truc, and P. T. B. Nghi, "Studies on chemical, polyphenol content, flavonoid content, and antioxidant activity of sweet basil leaves (*Ocimum basilicum L.*)," in *IOP conference series: Materials Science and Engineering*, IOP Publishing, 2021.

[17] I. M. Janah, R. Roto, and D. Siswanta, "Very stable EDTA-stabilized colloidal silver nanoparticles: the role of synthesis parameters," *J. Photopolym. Sci. Technol.*, pp. 587–595, Jan 2021, doi: 10.2494/photopolymer.34.587.

[18] T. M. Kiio and S. Park, "Physical properties of nanoparticles do matter," *J Pharm Investig*, vol. 51, no. 1, pp. 35–51, Oct 2020, doi: 10.1007/s40005-020-00504-w.

[19] A. M. El-Khawaga, A. Zidan, and A. I. A. Abd El-Mageed, "Preparation methods of different nanomaterials for various potential applications: A review," *J Mol Struct*, vol. 1281, pp. 135148, Feb 2023, doi: 10.1016/j.molstruc.2023.135148.

[20] R. Singh, P. Thakur, A. Thakur, H. Kumar, P. Chawla, J. V. Rohit, R. Kaushik, and N. Kumar, "Colorimetric sensing approaches of surface-modified gold and silver nanoparticles for detection of residual pesticides: a review," *Int J Environ Anal Chem*, vol. 101, no. 15, pp. 3006–3022, Jan 2020, doi: 10.1080/03067319.2020.1715382.

[21] I. I. Ozyigit, I. Dogan, A. H. Ozyigit, B. Yalcin, A. Erdogan, I. E. Yalcin, E. Cabi, and Y. Kaya, "Production of secondary metabolites using tissue culture-based biotechnological applications," *Front Plant Sci*, vol. 14, pp. 1132555, Jun 2023, doi: 10.3389/fpls.2023.1132555.

[22] O. S. Teniola, A. A. Adeleke, S. A. Ibitoye, and M. D. Shittu, "Production of a highly concentrated gold solution from aqua regia gold leachate using sugarcane bagasse nanoparticles," *Hungarian Journal of Industry and Chemistry*, vol. 51, no. 2, pp. 27–33, Nov 2023, doi: 10.33927/hjic-2023-15

[23] J. Dong, P. L. Carpinone, G. Pyrgiotakis, P. Demokritou, and B. M. Moudgil, "Synthesis of precision gold nanoparticles using Turkevich method," *KONA Powder and Particle Journal*, vol. 37, pp. 224–232, 2020, doi: 10.14356/kona.2020011.

[24] J. K. Young, N. A. Lewinski, R. J. Langsner, L. C. Kennedy, A. Satyanarayan, V. Nammalvar, A. Y. Lin, and R. A. Drezek, "Size-controlled synthesis of monodispersed gold nanoparticles via carbon monoxide gas reduction," *Nanoscale Res Lett*, vol. 6, pp. 428, Jun 2011, doi: 10.1186/1556-276X-6-428.

[25] D. Subara and I. Jaswir, "Gold nanoparticles: Synthesis and application for halal authentication in meat and meat products," *Int J Adv Sci Eng Inf Technol*, vol. 8, no. 4–2, pp. 1633–1641, Jul 2018, doi: 10.18517/ijaseit.8.4-2.7055.

[26] S. Sangwan and R. Seth, "Synthesis, characterization and stability of gold nanoparticles (AuNPs) in different buffer systems," *J Clust Sci*, vol. 33, no. 2, pp. 749–764, Mar 2022, doi: 10.1007/s10876-020-01956-8.

[27] P. Khajegi and M. Rashidi-Huyeh, "Optical properties of gold nanoparticles: shape and size effects," *International Journal of Optics and Photonics*, vol. 15, no. 1, pp. 41–48, Jan 2021, doi: 10.52547/ijop.15.1.41.

[28] E. A. Lelah, M. Karim, and Y. Fatemeh, "The pH role in nanotechnology, electrochemistry, and nano-drug delivery," *J. Chem. Chem. Eng. Research Article*, vol. 41, no. 7, pp. 2175–2188, Jul 2022, doi: 10.30492/ijcce.2022.121271.4009.

[29] R. Pranata Putri, S. Oktavia Nur Yudiastuti, "Green synthesis dan karakterisasi nanopartikel emas (AuNPs) menggunakan asam askorbat dan iradiasi sinar UV," *Jurnal Kolaboratif Sains*, vol. 7, no. 2, pp. 621–629, Feb 2024, doi: 10.56338/jks.v7i2.4717.

[30] S. Annur, S. J. Santosa, and N. H. Aprilita, "pH dependence of size control in gold nanoparticles synthesized at room temperature," *Oriental Journal of Chemistry*, vol. 34, no. 5, pp. 2305–2312, Oct 2018, doi: 10.13005/ojc/340510.

[31] P. Pourali, O. Benada, M. Pátek, E. Neuhöferová, V. Dzmitruk, and V. Benson, "Response of biological gold nanoparticles to different pH values: is it possible to prepare both negatively and positively charged nanoparticles?," *Applied Sciences*, vol. 11, pp. 11559, Dec 2021, doi: 10.3390/app112311559.

[32]]N. I. Farihah and T. Taufikurohmah, "Green synthesis gold nanoparticles using bioreductant red shoot leaf extract (*Syzygium myrtifolium Walp*.) and activity as antioxidant," *Jurnal Pijar Mipa*, vol. 19, no. 4, pp. 746–752, Jul 2024, doi: 10.29303/jpm.v19i4.7171.

[33] C. Chen, S. Yang, Y. Liu, Y. Qiu, and J. Yao, "Metal ions-bridged J-aggregation mediated nanoassembly composition for breast cancer phototherapy," *Asian J Pharm Sci*, vol. 17, no. 2, pp. 230–240, Mar 2022, doi: 10.1016/j.ajps.2022.01.003.

[34] S. Pedroso-Santana and N. Fleitas-Salazar, "The use of capping agents in the stabilization and functionalization of metallic nanoparticles for biomedical applications," *Particle & Particle Systems Characterization*, vol. 40, no. 2, pp. 2200146, Dec 2022, doi: 10.1002/ppsc.202200146.

[35] S. Ali, M. Iqbal, A. Naseer, M. Yaseen, I. Bibi, A. Nazir, M. I. Khan, N. Tamam, N. Alwadai, M. Rizwan, and M. Abbas, "State of the art of gold (Au) nanoparticles synthesis via green routes and applications: A review," Environmental Nanotechnology, Monitoring & Management, vol. 16, Dec 2021, doi: 10.1016/j.enmm.2021.100511.

[36] P. Szczyglewska, A. Feliczak-Guzik, and I. Nowak, "Nanotechnology–general aspects: A chemical reduction approach to the synthesis of nanoparticles," *Molecules*, vol. 28, no. 13, pp. 4932, Jun 2023, doi: 10.3390/molecules28134932.

[37] K. K. Bharadwaj, B. Rabha, S. Pati, T. Sarkar, B. K. Choudhury, A. Barman, D. Bhattacharjya, A. Srivastava, D. Baishya, H. A. Edinur, Z. A. Kari, and N. H. M. Noor, "Green synthesis of gold nanoparticles using plant extracts as beneficial prospect for cancer theranostics," *Molecules*, vol. 26, no. 21, pp. 6389, Oct 2021, doi: 10.3390/molecules26216389.

[38] N. Baig, I. Kammakakam, and W. Falath, "Nanomaterials: A review of synthesis methods, properties, recent progress, and challenges," *Mater Adv*, vol. 2, no. 6, pp. 1821–1871, Mar 2021, doi: 10.1039/d0ma00807a.

[39] B. Islam, D. Samir, C. Sara, and N. Janetta, "*Ocimum basilicum L.* leaves extract-mediated green synthesis of MnO NPs: Phytochemical profile, characterization, catalytic and thrombolytic activities," *Results in Surfaces and Interfaces*, vol. 17, pp. 100284, Oct 2024, doi: 10.1016/j.rsurfi.2024.100284.

[40]]S. Patra, A. K. Golder, and R. V. S. Uppaluri, "Monodispersed AuNPs synthesized in a bio-based route for ultra selective colorimetric determination of Ni (II) ions," *Chemical Physics Impact*, vol. 7, pp. 100388, Dec 2023, doi: 10.1016/j.chphi.2023.100388.

[41] A. Marfina, E. Cahyono, S. Mursiti, and H. Harjono, "Sintesis nanopartikel emas dengan bioreduktor minyak atsiri kayu manis (*Cinnamomum Burmannii*)," *Indonesian Journal of Chemical Science*, vol. 8, no. 2, pp. 126–132, 2019.

[42] M. H. Shahrajabian, W. Sun, and Q. Cheng, "Chemical components and pharmacological benefits of Basil (*Ocimum basilicum*): A review," *Int J Food Prop*, vol. 23, no. 1, pp. 1961–1970, Nov 2020, doi: 10.1080/10942912.2020.1828456.

[43] Y. Faramitha, F. Dimawarnita, H. T. Prakoso, and Siswanto, "Sintesis, karakterisasi, dan pengujian aktivitas antifungi nanopartikel perak–cysteine secara in vitro terhadap *Ganoderma boninense*," *Menara Perkeb*, vol. 90, no. 2, pp. 81–89, Sep 2022, doi: 10.22302/iribb.jur.mp.v90i2.501.

[44] R. S. Nijhu, A. Khatun, and M. F. Hossen, "A comprehensive review of particle size analysis techniques," *International Journal of Pharmaceutical Research and Development*, vol. 6, no. 1, pp. 1–5, Jan 2024, doi: 10.33545/26646862.2024.v6.i1a.37.

[45] J. Zhao, Y. Ruan, Z. Zheng, Y. Li, M. Sohail, F. Hu, J. Ling, and L. Zhang, "Gold nanoparticles-anchored peptides enable precise colorimetric estimation of microplastics," *iScience*, vol. 26, no. 6, Jun 2023, doi: 10.1016/j.isci.2023.106823.

[46] J. Hong, B. Lee, C. Park, and Y. Kim, "A colorimetric detection of polystyrene nanoplastics with gold nanoparticles in the aqueous phase," *Science of the Total Environment*, vol. 850, Dec 2022, doi: 10.1016/j.scitotenv.2022.158058.

[47] A. Prajapati, A. Narayan Vaidya, and A. R. Kumar, "Microplastic properties and their interaction with hydrophobic organic contaminants: a review," *Environmental Science and Pollution Research*, vol. 29, no. 33, pp. 49490–49512, May 2022, doi: 10.1007/s11356-022-20723-y.

[48] L. Ding, Y. Luo, X. Yu, Z. Ouyang, P. Liu, and X. Guo, "Insight into interactions of polystyrene microplastics with different types and compositions of dissolved organic matter," *Science of the Total Environment*, vol. 824, pp. 153883, Jun 2022, doi: 10.1016/j.scitotenv.2022.153883.

[49] J. Hong, B. Lee, C. Park, and Y. Kim, "A colorimetric detection of polystyrene nanoplastics with gold nanoparticles in the aqueous phase," *Science of the Total Environment*, vol. 850, pp. 158058, Dec 2022, doi: 10.1016/j.scitotenv.2022.158058.

[50] P. M. Nowak, "What does it mean that 'something is green'? The fundamentals of a unified greenness theory," *Royal Society of Chemistry*, vol. 12, no. 12, pp. 4625-4640, May 2023, doi: 10.1039/d3gc00800b.

[51] J. B. Zimmerman, P. T. Anastas, H. C. Erythropel, and W. Leitner, "Designing for a green chemistry future," *Chemistry For Tomorrow's Earth*, vol. 367, no. 1, pp. 397–400, Jan 2020, doi: 10.1126/science.aay3060.

[52] M. B. Thohir, "Penerapan green chemistry nomor 7 untuk penurunan kesadahan air," *Hydrogen: Jurnal Kependidikan Kimia*, vol. 11, no. 6, pp. 874, Dec 2023, doi: 10.33394/hjkk.v11i6.9871.

[53] M. B. Thohir, R. Roto, and S. Suherman, "A Sol-gel membrane utilized cellulose paper doped with α-furil dioxime for colorimetric determination of nickel," *Bull Environ Contam Toxicol*, vol. 109, no. 6, pp. 1183–1189, Dec 2022, doi: 10.1007/s00128-022-03622-3.

[54] G. Suriyakala, S. Sivaji, R. Babujanarthanam, K. Mohammed, D. S. Hussein, R. A. Rasheed, and K. Kanimozhi, "Green synthesis of gold nanoparticles using Jatropha integerrima Jacq. flower extract and their antibacterial activity," *J King Saud Univ Sci*, vol. 34, no. 3, Apr 2022, doi: 10.1016/j.jksus.2022.101830.